Inorg. Chem. **1999,** *38,* 3787−3795

Quercetin 2,3-Dioxygenase Mimicking Ring Cleavage of the Flavonolate Ligand Assisted by Copper. Synthesis and Characterization of Copper(I) Complexes [Cu(PPh$_3$)$_2$(fla)] (fla = Flavonolate) and [Cu(PPh$_3$)$_2$(*O*-bs)] (*O*-bs = *O*-Benzoylsalicylate)

Éva Balogh-Hergovich,[1a] József Kaizer,[1b] Gábor Speier,*,[1b] Vilmos Fülöp,[1c] and László Párkányi[1c]

Department of Organic Chemistry, University of Veszprém, 8201 Veszprém, Hungary, Research Group for Petrochemistry of the Hungarian Academy of Sciences 8201 Veszprém, Hungary, and Central Research Institute of Chemistry of the Hungarian Academy of Sciences, 1525 Budapest, Hungary

Received February 12, 1999

Cu(PPh$_3$)$_2$(fla) has been prepared by reacting copper(I) chloride with sodium flavonolate in tetrahydrofuran solution. Crystallographic characterization of the complex (orthorhombic, $P2_12_12_1$, $a = 9.588(1)$ Å, $b = 17.364(3)$ Å, $c = 24.378(3)$ Å, $V = 4058.6(10)$ Å^3, $Z = 4$, $R = 0.049$) has shown that the coordination geometry of the molecule is tetrahedral. Oxygenation of Cu(PPh$_3$)$_2$(fla) in a methylene chloride solution at ambient conditions gives the *O*-benzoylsalicylato copper complex Cu(PPh$_3$)$_2$(*O*-bs) and carbon monoxide. Labeling experiments with an $^{18}O_2$−$^{16}O_2$ mixture (1:4) evidenced the incorporation of both ^{18}O atoms of $^{18}O_2$ into the *O*-bs ligand. IR and MS studies of labeled *O*-bs confirmed the incorporation of $^{18}O_2$ while the released CO remained unlabeled. Crystallographic characterization of Cu(PPh$_3$)$_2$(*O*-bs) on crystals obtained as the acetone solvate (triclinic, $P\bar{1}$, $a = 13.154(1)$ Å, $b = 17.991(1)$ Å, $c = 20.495(1)$ Å, $\alpha = 80.01(1)°$, $\beta = 88.02(1)°$, $\gamma = 71.83(1)°$, $V = 4537.5(5)$ Å^3, $Z = 4$, $R = 0.0403$) shows that the molecule has a distorted tetrahedral structure. The oxygenolysis was followed by spectrophotometry, and the rate constants were determined according to the rate law $-d[\mathrm{Cu(PPh_3)_2(fla)}]/dt = k_2[\mathrm{Cu(PPh_3)_2(fla)}][\mathrm{O_2}]$. The rate constant, activation enthalpy, and entropy at 363.16 K are as follows: $k_2/\mathrm{M^{-1}\,s^{-1}} = 4.16 \pm 0.48$, $\Delta H^{\ddagger}/\mathrm{kJ\,mol^{-1}} = 102 \pm 7$, $\Delta S^{\ddagger}/\mathrm{J\,mol^{-1}\,K^{-1}} = -13.0 \pm 21$. The reaction fits a Hammett linear free energy relationship for 4′-substituted flavonolates, and an increase of the electron density on copper makes the oxygenation reaction faster.

Introduction

The fundamental nature of metalloenzymes is being widely studied. Biological and biomimetic works aim to elucidate and understand the structure of these enzymes and specially the role of metal ions in the enzymatic process. Many of these metalloenzymes, containing mainly iron or copper ions at their active site, utilize molecular oxygen for the metabolism of organic substrates.[2−9] Modeling studies on the activation of dioxygen and/or substrates of these enzymes may contribute to our understanding of the mechanistic feature of these processes.[10,11] The dioxygen chemistry of copper[12−18] and iron[19,20] and the coordination chemistry of some of the substrates help in understanding the catalytic factors for enhanced reactivities. There is vivid interest in iron and copper-containing monooxygenase[21−23] and dioxygenase enzymes[24−27] and in their structural and functional model systems. It has been shown that in the case of catechol dioxygenase models of copper[28] and

---

(1) (a) Research Group for Petrochemistry of the Hungarian Academy of Sciences. (b) University of Veszprém. (c) Central Research Institute of Chemistry of the Hungarian Academy of Sciences.

(2) Fox, B. G.; Lipscomb, J. D. In *Biological Oxidation Systems;* Reddy, C.; Hamilton, G. A., Eds.; Academic Press: New York, 1990; Vol. 1, pp 367−388.

(3) Karlin, K. D.; Tyeklár, Z. *Bioinorganic Chemistry of Copper*; Chapman & Hall: New York, 1992.

(4) Solomon, E. I.; Baldwin, M. J.; Lowery, M. D. *Chem. Rev.* **1992**, *92*, 521.

(5) Karlin, K. D. *Science* **1993**, *261*, 701.

(6) Levine, W. G. In *The Biochemistry of Copper*; Peisach, J., Aisen, P., Blumberg, W. E., Eds.; Academic Press: New York, 1966; pp 371−387.

(7) Halfen, J. A.; Mahapatra, S.; Wilkinson, E. C.; Kaderli, S.; Young, V. G.; Que, L., Jr.; Zuberbühler, A. D.; Tolman, W. B. *Science* **1996**, *271*, 1397.

(8) Vincent, J. B.; Olivier-Lilley, G. L.; Averill, B. A. *Chem. Rev.* **1990**, *90*, 1447.

(9) Waltar, B. J.; Lipscomb, J. D. *Chem. Rev.* **1996**, *96*, 2625.

(10) *Catalysis by Metal Complexes*, *Oxygenases and Model Systems*; Funabiki, T., Ed.; Kluwer Academic Press: Dordrecht, The Netherlands, 1997; Vol. 19.

(11) Sono, M.; Roach, M. P.; Coulter, E. D.; Dawson, J. H. *Chem. Rev.* **1996**, *96*, 2841.

(12) Karlin, K. D.; Kaderli, S.; Zuberbühler, A. D. *Acc. Chem. Res.* **1997**, *30*, 139.

(13) Karlin, K. D.; Tyeklár, Z.; Zuberbühler, A. D. In *Bioinorganic Catalysis*; Reedijk, J., Ed.; Marcel Dekker: New York, 1993; pp 261−315.

(14) Mahapatra, S.; Halfen, J. A.; Wilkinson, E. C.; Pan, G.; Wang, X.; Young, J. V. G.; Cramer, C. J.; Que, L., Jr.; Tolman, W. B. *J. Am. Chem. Soc.* **1996**, *118*, 11555.

(15) Mahapatra, S.; Young, J. V. G.; Kaderli, S.; Zuberbühler, A. D.; Tolman, W. B. *Angew. Chem., Int. Ed. Engl.* **1997**, *36*, 130.

(16) Mahadevan, V.; Hou, Z.; Cole, A. P.; Root, D. E.; Lal, T. K.; Solomon, E. I.; Stack, T. D. P. *J. Am. Chem. Soc*. **1997**, *119*, 11996.

(17) Obias, H. V.; Lin, Y.; Murthy, N. N.; Pidcock, E.; Solomon, E. I.; Ralle, M.; Blackburn, N. J.; Neuhold, Y. M.; Zuberbühler, A. D.; Karlin, K. D. *J. Am. Chem. Soc.* **1998**, *120*, 12960.

(18) Tolman, W. B. *Acc. Chem. Res.* **1997**, *30*, 227.

(19) Kurtz, D. M., Jr. *Chem. Rev.* **1990**, *90*, 585.

(20) Que, L., Jr. *J. Chem. Soc., Dalton Trans.* **1997**, 3933.

(21) Nguyen, H.-H. T.; Shiemke, A. K.; Jacobs, S. J.; Hales, B. J.; Lidstrom, M. E.; Chan, S. I. *J. Biol. Chem.* **1994**, *269*, 14995.

10.1021/ic990175d CCC: $18.00

Scheme 1

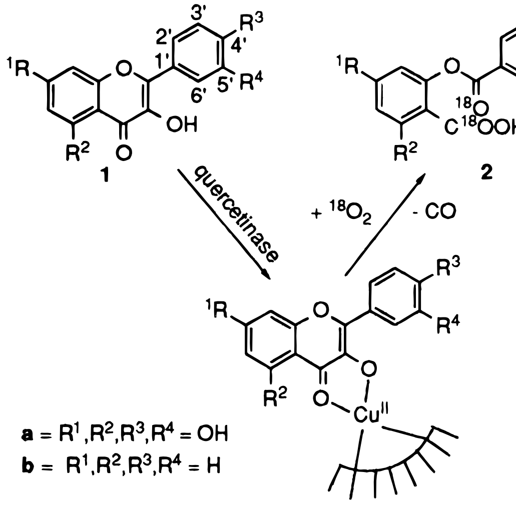

iron[29] the oxidative intradiol cleavage of catecholates to muconic acids proceeds through intramolecular redox steps, involving catecholate (cat.) and semiquinone (SQ) ligands coupled with metal ions of varying oxidation state (eqs 1 and 2). They are

$$\mathrm{Fe^{III}(cat.) \rightleftharpoons Fe^{II}(SQ)} \tag{1}$$

$$\mathrm{Cu^{II}(cat.) \rightleftharpoons Cu^{I}(SQ)} \tag{2}$$

believed to be responsible for substrate activation. In these reactions $\mathrm{Fe^{II}}$ or $\mathrm{Cu^{I}}$ and also the semiquinone ligand (SQ) may react with dioxygen at ambient conditions.[30,31] Both substrate activation (intradiol cleavage) and dioxygen activation (extradiol cleavage in the case of iron) have been established for the mechanism of the enzyme reaction.[32]

In the microbial metabolism of rutin by *Aspergillus* or *Pulmallaria* species, quercetin (3′,4′,5,7-tetrahydroxyflavonol, **1a**) is oxidatively degraded into a depside (phenolic carboxylic acid ester, **2**) and carbon monoxide[33−38] (Scheme 1). It has been found that the copper-containing quercetin 2,3-dioxygenase is responsible for the oxidative process.[37] Labeling experiments with $^{18}\mathrm{O}_2$ proved the incorporation of both $^{18}\mathrm{O}$ atoms into the substrate which is characteristic of dioxygenases.[38] Purification and characterization of the enzyme showed the copper to be in the oxidation state $\mathrm{Cu^{II}}$, but the ligand environment around $\mathrm{Cu^{II}}$ has not been determined. Quercetin is believed to coordinate to copper through the 3-hydroxy and 4-carbonyl groups.[39−41]

Model oxygenation reactions on quercetin and the parent compound flavonol (**1b**) have been carried out in order to understand the enzymic reaction. Base-catalyzed oxygenation of quercetin and related 3-hydroxyflavones under aqueous[42] and nonaqueous[43] conditions, photosensitized oxygenations,[44] and reactions with superoxide[45] have been investigated. Metal complexes of cobalt[46−48] and copper[49−51] have been found to act as catalysts for the oxygenation reaction. Copper(I)[52] and copper(II)[53] flavonolate complexes were also successfully used for the oxygenation of flavonol.

Recent crystallographic studies of flavonolato complexes of copper(I),[52] copper(II),[53] cobalt(III),[54] and zinc(II)[55] disclosed the coordination mode of the flavonolate ligand, geometries around the metal ions, and their influence on the delocalization of π-electrons in the flavonolate ligand.

We have been concerned with the synthesis of copper flavonolates and quercetin 2,3-dioxygenase mimicking oxygenations.[56−58] By the use of simple ligands we aimed to work on synthetic analogues and synthesize stable flavonolato and quercetin complexes of copper suitable for structural characterization which bear close resemblance to the enzyme. In the present paper, we report details for the synthesis and characterization of $\mathrm{Cu(PPh_3)_2(fla)}$ (fla = flavonolate, **3**) and its oxygenated product $\mathrm{Cu(PPh_3)_2(}$*O*-bs) (*O*-bs = *O*-benzoylsalicylate, **4**), and details of the oxidative ring cleavage reaction supported by $^{18}\mathrm{O}$-labeling and kinetic experiments.

Experimental Section

Materials and Methods. Solvents used for the reactions were purified by literature methods[59] and stored under argon. 3-Hydroxyflavone,[42] 3,4′-dihydroxyflavone,[42] 3-hydroxy-4′-methylflavone,[60] 3-hy-

---

(22) Chan, S. I.; Nguyen, H.-H. T.; Shiemke, A. K.; Listrom, M. E. In *Bioinorganic Chemistry of Copper*; Karlin, K. D., Tyeklár, Z., Eds.; Chapman & Hall: New York, 1992; pp 184−195.

(23) Blackburn, N. J. In *Bioinorganic Chemistry of Copper*; Karlin, K. D., Tyeklár, Z., Eds.; Chapman & Hall: New York, 1992; pp 164−183.

(24) Nair, P. M.; Vadyanathan, C. S. *Biochim. Biophys. Acta* **1964**, *81*, 496.

(25) Brady, F. O. *Bioinorg. Chem.* **1975**, *5*, 167.

(26) Hayaishi, O. *Bacteriol. Rev.* **1966**, *30*, 720.

(27) Speier, G. *New J. Chem.* **1994**, *18*, 143.

(28) Speier, G.; Tyeklár, Z.; Szabó, L., II; Tóth, P.; Pierpont, C. G.; Hendrickson, D. N. Evidences for Substrate Activation of Copper Catalyzed Intradiol Cleavage in Catechols. In *The Activation of Dioxygen and Homogeneous Catalytic Oxidation;* Barton, D. H. R., Martell, A. E., Sawyer, D. T., Eds.; Plenum Press: New York, 1993; pp 423−436.

(29) Que, L., Jr.; Ho, R. Y. N. *Chem. Rev.* **1996**, *96*, 2607.

(30) (a) Pierpont, C. G.; Lange, C. W. *Prog. Inorg. Chem.* **1994**, *41*, 331.

(31) Jang, H. G.; Cox, D. D.; Que, L., Jr. *J. Am. Chem. Soc.* **1991**, *113*, 9200.

(32) Funabiki, T.; Mizoguchi, A.; Sugimoto, T.; Tada, S.; Tsuji, M.; Sakamoto, H.; Yoshida, S. *J. Am. Chem. Soc.* **1986**, *108*, 2921.

(33) Westlake, D. W.; Talbot, G.; Blakely, E. R.; Simpson, F. J. *Can J. Microbiol.* **1959**, *5*, 62.

(34) Simpson, F. J.; Talbot, G.; Westlake, D. W. S. *Biochem. Biophys. Res. Commun.* **1959**, *2*, 621.

(35) Hattori, S.; Noguchi, I. *Nature* **1959**, *184*, 1145.

(36) Sakamoto, H. *Seikagu (J. Jpn. Biochem. Soc.)* **1963**, *35*, 633.

(37) Oka, T.; Simpson, F. J.; Krishnamurty, H. G. *Can. J. Microbiol.* **1977**, *16*, 493.

(38) Krishnamurty, H. G.; Simpson, F. J. *J. Biol. Chem.* **1970**, *245*, 1476.

(39) Makasheva, E.; Golovkina, N. T. *Zh. Obsch. Khim.* **1973**, *43*, 1640.

(40) Thomson, M.; Williams, C. R. *Anal. Chim. Acta* **1976**, *85*, 375.

(41) Takamura, K.; Ito, M. *Chem. Pharm. Bull.* **1977**, *25*, 3218.

(42) Nishinaga A.; Tojo, T.; Tomita, H.; Matsuura, T. *J. Chem. Soc., Perkin Trans. 1* **1979**, 2511.

(43) Rajananda, V.; Brown, S. B. *Tetrahedron Lett.* **1981**, *22*, 4331.

(44) Matsuura, T.; Matsushima, H.; Nakashima, R. *Tetrahedron Lett.* **1970**, *26*, 435.

(45) El-Sukkary, M. M. A.; Speier, G. *J. Chem. Soc., Chem. Commun.* **1981**, 745.

(46) Nishinaga, A.; Tojo, T.; Matsuura, T. *J. Chem. Soc., Chem. Commun.* **1974**, 896.

(47) Nishinaga, A.; Numada, N.; Maruyama, K. *Tetrahedron Lett.* **1989**, *30*, 2257.

(48) Nishinaga, A.; Kuwashige, T.; Tsutsui, T.; Mashino, T.; Maruyama, K. *J. Chem. Soc., Dalton Trans.* **1994**, 805.

(49) Utaka, M.; Hojo, M.; Fujii, Y.; Takeda, A. *Chem. Lett.* **1984**, 635.

(50) Utaka, M.; Takeda, A. *J. Chem. Soc., Chem. Commun.* **1985**, 1824.

(51) Balogh-Hergovich, É.; Speier, G. *J. Mol. Catal.* **1992**, *71*, 1.

(52) Speier, G.; Fülöp, V.; Párkányi, L. *J. Chem. Soc., Chem. Commun.* **1990**, 512.

(53) Balogh-Hergovich, É.; Speier, G.; Argay, G. *J. Chem. Soc., Chem. Commun.* **1991**, 551.

(54) Hiller, W.; Nishinaga, A.; Rieker, A. *Z. Naturforsch.* **1992**, *47b*, 1185.

(55) Annan, T. A.; Peppe, C.; Tuck, D. G. *Can. J. Chem.* **1990**, *68*, 423.

(56) Lippai, I.; Speier, G.; Huttner, G.; Zsolnai, L. *Chem. Commun.* **1997**, 741.

(57) Lippai, I.; Speier G. *J. Mol. Catal.* **1998**, *130*, 139.

(58) Lippai, I.; Speier, G.; Huttner, G.; Zsolnai, L. *Acta Crystallogr.* **1997**, *C53*, 1547.

(59) Perrin, D. D.; Armarego, W. L.; Perrin, D. R. *Purification of Laboratory Chemicals,* 2nd ed.; Pergamon: New York, 1990.

Table 1. Physical Properties and Analyses of Complexes $Cu(PPh_3)_2$(4′-R-fla) (**3a**−**e**)

cmpd	R	yield, %[a]	color	mp, °C	C, %		H, %	
					calcd	found	calcd	found
3a	H	88	orange	153−155	74.21	74.30	4.76	4.67
3b	OH	84	pink	63−65	72.81	73.10	4.67	4.59
3c	CH_3	82	orange	142−147	74.41	74.18	4.92	4.84
3d	NO_2	76	orange	>300	70.37	70.11	4.40	4.30
3e	Cl	84	orange	68−70	71.24	70.92	4.45	4.53

[a] Isolated yields.

Table 2. Characteristic Absorption Bands of Complexes $Cu(PPh_3)_2$(4′-R-fla) (**3a**−**e**)

complex	R	$\nu_{(C=O)}$ [cm^{-1}] (Nujol)	$\Delta\nu_{(C=O)}$ [cm^{-1}]	UV−vis (DMF) λ[nm] (log ϵ)	
3a	H	1554	54	266.5 (4.38)	430.5 (3.89)
3b	OH	1549	52	265.0 (4.45)	440.5 (3.95)
3c	Me	1548	67	263.5 (4.39)	436.0 (3.87)
3d	NO_2	1549	66	270.5 (4.30)	417.5 (3.88)
3e	Cl	1549	66	263.0 (4.31)	430.5 (3.60)

droxy-4′-chloroflavone,[60] 3-hydroxy-4′-nitroflavone,[61] and *O*-benzoylsalicylic acid[62] were prepared by literature methods. CuCl obtained from Reanal (reagent grade) was washed with acetic acid on a filter several times until the filtrate became colorless. The resulting white solid was subsequently treated with distilled water, dried under vacuum, and stored in a Schlenck tube under an atmosphere of argon. A sample of $^{18}O_2$ was purchased from Pierce Inorganics B. V. Other reagents were the highest grade commercially available and were used without further purification. Diazomethane[63] was freshly prepared according to the literature in ether and immediately used for the methylation reactions. All reactions were performed by standard Schlenck technics under argon.[64]

$Cu(PPh_3)_2$(fla) (3a). To a stirred solution of flavonol (2.38 g, 10 mmol) in anhydrous tetrahydrofuran (100 mL) was added sodium (0.23 g, 10 mmol) under argon. After dissolution of the sodium, triphenylphosphine (5.25 g, 20 mmol) and CuCl (1.0 g, 10 mmol) were added. The mixture was stirred for 1 h, the solvent was evaporated in a vacuum, and the residue was treated with ether and recrystallized from ether to give orange diamagnetic crystals of **3a** suitable for X-ray diffraction experiments (7.26 g, 88%): mp 153−155 °C; UV−vis (λ_{max}, CH_2Cl_2) 232 nm (log ϵ 4.89), 272 (4.54), 426 (3.88); IR (Nujol) 1583, 1554, 1487, 1473, 1440, 1413, 1323, 1227, 1087, 1031, 1000, 757, 700, 521, 513, 493 cm^{-1}; ^1H NMR ($CDCl_3$, 22 °C) δ 7.19−8.44 (m, ArH); ^{31}P NMR ($CDCl_3$, 22 °C) δ 29.62; ^{13}C NMR ($CDCl_3$, 22 °C) δ 161.8, 154.9, 145.1, 134.3, 134.0, 133.3, 132.5, 132.2, 132.0, 131.9, 129.3, 128.9, 128.6, 128.4, 127.8, 127.2, 125.4, 123.6, 120.8, 118.1; ^{13}C NMR (DMSO-d_6, 30 °C) δ 174.6, 162.2, 154.6, 145.1, 141.8, 133.7, 133.5, 132.5, 131.7, 131.6, 129.7, 129.5, 128.9, 128.7, 128.5, 127.4, 124.8, 124.5, 118.5.

Anal. Calcd for $C_{51}H_{39}O_3CuP_2$: C, 74.21; H, 4.76. Found C, 74.30; H, 4.67.

$Cu(PPh_3)_2$(4′R-fla) (3b−e). Complexes **3b**−**e** were prepared by the same method as that described above for the preparation of **3a**. Properties, analyses, and IR and UV−vis data of the complexes are summarized in Tables 1 and 2.

Cu(*O*-bs)$_2$·C_2H_5OH (5). To a solution of $Cu(OAc)_2$·$2H_2O$ (2.00 g, 10 mmol) in ethanol (80 mL) was added benzoylsalicylic acid (4.84 g, 20 mmol) in ethanol (20 mL) with stirring at 40 °C. The solution was stirred for 3 h and allowed to cool to room temperature. The blue crystalline product was collected by filtration, washed with ethanol, and dried under vacuum (5.12 g, 86%): IR (Nujol) 3614, 1740, 1627, 1447, 1406, 1256, 1207, 1094, 1056, 1014, 774, 700 cm^{-1}.

Anal. Calcd for $C_{30}H_{24}O_9Cu$: C, 60.85; H, 4.08. Found C, 60.55; H, 3.97.

$Cu(PPh_3)_2$(*O*-bs) (4a). Method A. Flavonolatobis(triphenylphosphine)copper(I) (0.82 g 1.0 mmol) in methylene chloride (10 mL) was treated with dioxygen (0.1 MPa) at room temperature for 30 h (27 mL, 1.08 mmol) yielding a pale yellow solution. This was evaporated to dryness giving a light yellow residue (0.65 g, 78%): mp 148−150 °C; IR (Nujol) 1734, 1587, 1547, 1464, 1435, 1380, 1267, 1200, 1100, 1067, 1027, 752, 700, 516, 500 cm^{-1}.

Anal. Calcd for $C_{50}H_{39}O_4P_2Cu$: C, 72.4; H, 4.74. Found C, 71.83; H, 4.82.

Method B. Cu(*O*-bs)$_2$·C_2H_5OH (5.97 g, 10 mmol) and triphenylphosphine (6.55 g, 25 mmol) were refluxed under argon in anhydrous MeOH (200 mL) for 3 h. The colorless solution was cooled to room temperature, evaporated to half volume under vacuum, and cooled in a refrigerator for several hours. The white precipitate was filtered off, washed with absolute methanol, and dried in a vacuum (7.1 g, 86%).

$Cu(PPh_3)_2$(*O*-bs)·CH_3COCH_3 (4a·CH_3COCH_3). Complex **4a** (0.414 g, 0.5 mmol) was dissolved in boiling acetone (15 mL), and after cooling, the solution colorless crystalline product was obtained (0.41 g, 92%): mp 180−182 °C; IR (KBr) 1738, 1710, 1584, 1551, 1476, 1429, 1393, 1267, 1196, 1093, 1059, 1023, 740, 694, 516, 505 cm^{-1}; UV−vis (λ_{max}, DMF) 264 nm (log ϵ 4.35); ^1H NMR ($CDCl_3$, 20 °C) δ 2.16 (s, 6H, CH_3), 7.05−7.45 (m, 38 H, ArH), 7.80−7.90 (m, 1H, ArH); ^{13}C NMR ($CDCl_3$, 22 °C) δ 206.8, 165.5, 149.8, 133.8, 133.7, 132.7, 132.4, 132.2, 131.5, 130.2, 129.7, 128.5, 127.8, 125.3, 122.9, 30.9; ^{13}C NMR (DMSO-d_6, 30 °C) δ 206.0, 170.2, 164.8, 149.9, 134.4, 134.2, 133.7, 133.5, 133.4, 131.6, 131.0, 130.3, 130.0, 129.7, 128.6, 125.5, 123.2, 31.0; ^{31}P NMR ($CDCl_3$, 22 °C) δ −3.2; ^{31}P NMR (DMSO-d_6, 22 °C) δ −6.16.

Anal. Calcd for $C_{53}H_{45}O_5P_2Cu$: C, 71.73; H, 5.11. Found C, 71.57; H, 5.16.

Instrumentation. IR spectra were recorded in either Nujol or KBr pellets on a Specord IR-75 (Carl Zeiss) spectrometer. Electronic spectra were measured on either a Specord M-40 (Carl Zeiss) or a Shimadzu UV-160 spectrometer using quartz cells. NMR spectra were recorded on a Varian Unity-300 spectrometer. ^1H NMR shifts are reported as values downfield from an external standard of Me_4Si. ^{13}C NMR spectra were obtained at 75.4 MHz, reference was the center peak of chloroform-*d* (77.0 ppm), or DMSO-d_6 (39.7 ppm). ^{31}P NMR spectra were recorded at 121.4 MHz with H_3PO_4 as external reference with downfield values reported as positive. The peak assignments were made using DEPT and APT methods. Magnetic susceptibility were determined by the Gouy method.[65] GC analyses were performed on a HP 5830A gas chromatograph equipped with a flame ionization detector and a CP SIL 8CB column. GC-MS measurements were recorded on a HP 5890II/5971 GC/MSD at 75 EV.

Kinetic Measurements. Reactions of $Cu(PPh_3)_2$(fla) with O_2 were performed in DMF solutions. In a typical experiment $Cu(PPh_3)_2$(fla) was dissolved under argon atmosphere in a thermostated reaction vessel with an inlet for taking samples with a syringe, and connected to mercury manometer to regulate constant pressure. The solution was then heated to the appropriate temperature. A sample was then taken by syringe, and the initial concentration of $Cu(PPh_3)_2$(fla) was determined by UV−vis spectroscopy measuring the absorbance of the reaction mixture at 430 nm (log ϵ 4.45) [λ_{max} of a typical band of $Cu(PPh_3)_2$(fla)]. The argon was then replaced with dioxygen, and the consumption of $Cu(PPh_3)_2$(fla) was analyzed periodically (ca. every 5 min). Experimental conditions are summarized in Table 3. The temperature was determined with an accuracy of ±0.5 °C; the concentrations of $Cu(PPh_3)_2$(fla) were measured with a relative mean error of ca. ±2%; the pressure of dioxygen was determined with an accuracy of ±0.5%. The O_2 concentration was calculated from literature data[66] taking into account the partial pressure of DMF[67] and assuming the validity of Dalton's law.

---

(60) Smith, M. A.; Newman, R. M.; Webb, R. A. *J. Heterocycl. Chem.* **1968**, *5*, 425.

(61) Reidel: L.; Hempel, G. *Justus Liebigs. Ann. Chem.* **1959**, *625*, 184.

(62) Einhorn, A.; Rothlauf, L.; Seuffert, R. *Chem. Ber.* **1911**, *44*, 3309.

(63) Arndt, F. In *Organic Syntheses*; Blatt, A. H., Ed.; John Wiley & Sons: New York, 1943; Vol. 2, p 165.

(64) Shriver, D. F.; Drezdzon, M. A. *The Manipulation of Air-sensitive Compounds;* John Wiley & Sons: New York, 1986.

(65) Carlin, R. L. *Magnetochemistry*; Springer-Verlag: Berlin, 1986; p 311.

(66) Kruis, A. In *Landolt-Börnstein*; Board 4, Teil 4., Springer-Verlag: Berlin, 1976; p 269.

(67) Ram, G.; Sharaf, A. R. *J. Ind. Chem. Soc.* **1968**, *45*, 13.

Table 3. Kinetic Data for the Oxygenation of $Cu(PPh_3)_2(fla)$ in DMF Solution

expt no.	temp, °C	$10^3[O_2]$, mol L^{-1}	$10^4[Cu]$, mol L^{-1}	$10^4k'$, s^{-1}	R, %[a]	10^3k, s^{-1} mol L^{-1}	$10^8d[Cu]/dt$, mol L^{-1} s^{-1}
1	90	1.96	2.02	0.06 ± 0.001	99.85	3.05 ± 0.05	0.12 ± 0.004
2	90	3.52	2.04	0.11 ± 0.003	99.43	3.01 ± 0.08	0.26 ± 0.008
3	90	5.93	2.04	0.26 ± 0.007	99.79	4.35 ± 0.12	0.62 ± 0.050
4	90	7.84	1.77	0.47 ± 0.016	99.31	5.99 ± 0.21	0.88 ± 0.071
5	90	9.01	1.94	0.56 ± 0.015	99.50	6.21 ± 0.17	1.09 ± 0.074
6	90	10.18	2.06	0.60 ± 0.003	99.81	5.89 ± 0.03	1.24 ± 0.036
7	90	12.52	2.06	0.82 ± 0.026	99.80	6.56 ± 0.21	1.69 ± 0.102
8	90	7.84	3.00	0.17 ± 0.003	99.82	2.20 ± 0.04	0.52 ± 0.008
9	90	7.84	5.00	0.30 ± 0.008	99.69	3.77 ± 0.10	1.48 ± 0.057
10	90	7.84	7.57	0.38 ± 0.004	99.94	4.90 ± 0.05	2.42 ± 0.065
11	90	7.84	10.00	0.18 ± 0.007	99.01	2.25 ± 0.09	2.72 ± 0.110
12	90	7.84	15.00	0.16 ± 0.007	99.36	1.98 ± 0.09	3.55 ± 0.119
						4.16 ± 0.48[b]	
13	100	7.70	1.96	1.05 ± 0.030	99.53	13.66 ± 0.40	
14	110	6.82	2.15	1.83 ± 0.083	99.28	26.82 ± 1.22	
15	120	6.06	2.20	3.82 ± 0.280	98.86	62.91 ± 4.62	

[a] Correlation coefficients of least-squares regressions. [b] Mean value of the kinetic constant k and its standard deviation $\sigma(k)$ were calculated as $k = (\sum_i w_i k_i/\sum_i w_i)$ and $\sigma(k) = (\sum_i w_i(k_i - k)^2/(n - 1)\sum_i w_i)^{1/2}$, where $w_i = 1/\sigma_i^2$.

Table 4. Crystallographic Data for $Cu(PPh_3)_2(fla)$ (**3a**) and $Cu(PPh_3)_2(O\text{-bs})\cdot CH_3COCH_3$[a] ($\mathbf{4a}\cdot CH_3COCH_3$)[a]

	3a	$\mathbf{4a}\cdot C_3H_6O$
formula	$C_{51}H_{39}CuO_3P_2$	$C_{53}H_{45}CuO_5P_2$
fw	825.30	887.37
cryst syst	orthorhombic	triclinic
space group	$P2_12_12_1$	$P\bar{1}$
a, Å	9.588(1)	13.154(1)
b, Å	17.364(3)	17.991(1)
c, Å	24.378(3)	20.495(1)
α, deg	90.000	80.01(1)
β, deg	90.000	88.02(1)
γ, deg	90.000	71.83(1)
V, Å^3	4058.6(10)	4537.5(5)
Z	4	4
temp, K	293(2)	293(2)
D_{calcd}, g cm^{-3}	1.351	1.299
$F(000)$	1712	1848
abs coeff, mm^{-1}	1.848	1.723
Θ range, deg	3.12−74.83	2.62−72.95
cryst size, mm	0.40 × 0.35 × 0.20	0.30 × 0.23 × 0.12
reflns collected	3358	18 134
independent refltns [R(int)=0.000]	3358	18 134
final R	0.0496	0.0403
final R_w	0.1238	0.1167
GOF on F^2	1.007	1.047

[a] Radiation Cu Kα (λ 1.541 84 Å); temp 293−298 K; $R = \Sigma||F_o| - |F_c||/\Sigma|F_o||$; $R_w = [\Sigma w(|F_o| - |F_c|)^2/\Sigma w|F_o|^2]^{1/2}$.

Crystallographic Structure Determinations $Cu(PPh_3)_2(fla)$. Crystals obtained from an ether solution formed as orange prisms. $Cu(PPh_3)_2(fla)$ indicated orthorhombic symmetry, and the centered settings of 25 reflections gave the unit cell dimensions listed in Table 4. Data were collected by ω/Θ scans on a Enraf-Nonius CAD-4 diffractometer within the angular range of 3.12−74.83°. The space group was found to be $P2_12_12_1$, and the structure was solved by the heavy atom method. Final cycles of refinement, including fixed contributions for the hydrogen atoms, converged with discrepancy indices of $R = 0.0496$ and $R_w = 0.1238$. Tables containing atom positions, anisotropic displacement parameters, hydrogen atom positions, bond lengths, and bond angles are available as Supporting Information.

$Cu(PPh_3)_2(O\text{-bs})$. Crystals obtained by recrystallization from acetone formed as colorless blocks. The complex indicated triclinic symmetry, and the centered settings of 25 reflections gave the unit cell dimensions listed in Table 4. Data were collected by ω/Θ scans on an Enraf-Nonius CAD-4 diffractometer within the angular range of 2.62−72.95°. The space group was found to be $P\bar{1}$, and the structure was solved by direct methods. Final cycles of refinement, including fixed contributions for the hydrogen atoms, converged with discrepancy indices of $R = 0.0403$ and $R_w = 0.1167$. Tables containing atom positions, anisotropic displacement parameters, hydrogen atom positions, bond lengths, and bond angles are available as Supporting Information.

Results

The sodium salt of flavonols react with cuprous chloride to give copper flavonolate complexes. In the presence of phosphine coligand tetrahedral $Cu^I(PR_3)_2(fla)$[52] products are obtained; with nitrogen-donor coligands octahedral $[Cu^I(fla)_3]^{2-}$ or planar $Cu(fla)_2$ products are formed.[56,53] Reactions carried out in the presence of triphenylphosphine have been found to give $Cu^I(PPh_3)_2(fla)$. In a similar way, starting from the sodium salt of 4′-chloro-, 4′-hydroxy-, 4′-methyl-, and 4′-nitroflavonol, the corresponding products obtained are $Cu(PPh_3)_2(4'\text{-R-fla})$. Characterization of the complexes is given in Tables 1 and 2. Oxygenation of $Cu(PPh_3)_2(fla)$ in dichloromethane solution at room temperature and 0.1 MPa dioxygen pressure have been found to give $Cu(PPh_3)_2(O\text{-bs})$ and carbon monoxide contaminated with a small amount of CO_2. Both complexes have been fully characterized, and the results of this investigation are described below.

$Cu(PPh_3)_2(fla)$. Crystallographic characterization has shown that $Cu(PPh_3)_2(fla)$ is tetrahedral. A view of the coordination geometry is given in Figure 1, and selected bond lengths and bond angles are listed in Table 5. It shows a distorted tetrahedral coordination geometry around the metal ions. The O(2)−Cu−O(3) angle within the chelate ring is 79.3(2)°, and the P(1)−Cu−P(2) angle is opened to 124.50(7)°. The Cu−O(3) bond length is 0.1 Å longer than the Cu−O(2) bond.

Copper oxygen bond distances are longer than those found in $[Cu_4(OBu^t)_4]$ [Cu−O$_{av}$ = 1.854(9) Å],[68] in $[Cu_2Cl_2(OMe)_2(py)_2]$ [1.932(4) and 1.940 Å],[69] and in $[Cu(PPh_3)_2(PhenSQ)]$ [2.082(7) and 2.111(8) Å].[70] The C(2)−O(2) distance is shorter while the C(3)−O(3) distance is longer than those in the uncoordinated flavonol [1.357(3) and 1.232(3) Å].[71] Due to coordination to the copper ion there is a change in the bond lengths of the pyranone ring. The O(1)−C(1) [1.369(3) Å] and C(1)−C(2) [1.363(4) Å] bond distances become longer, and the C(2)−C(3) bond distance [1.457(4) Å] shorter, which may be assigned to delocalization of the π-system over the whole molecule. The Cu−P bond distances are somewhat longer [Cu−

---

(68) Grezier, T.; Weiss, E. *Chem. Ber.* **1976**, *109*, 3142.
(69) Willett, R. D.; Breneman, G. L. *Inorg. Chem.* **1983**, *22*, 326.
(70) Speier, G.; Hendrickson, D. N. Unpublished results.
(71) Etter, M. C.; Urbanczyk-Lipkowska, Z.; Baer, S.; Barbara, P. F. *J. Mol. Struct.* **1986**, *144*, 155.

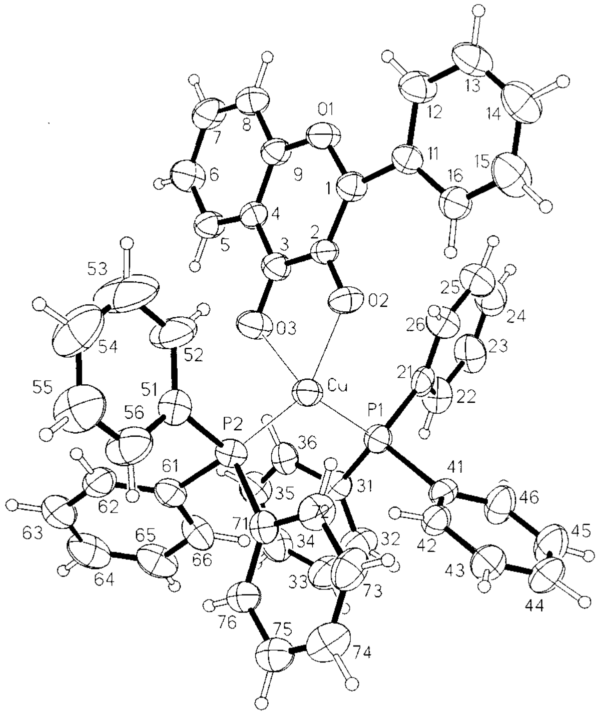

Figure 1. Molecular structure and atomic numbering scheme for $\mathrm{Cu(PPh_3)_2(fla)}$ (**3a**). Ellipsoids are drawn at the 50% probability level.

Table 5. Selected Bond Lengths and Angles for $\mathrm{Cu(PPh_3)_2(fla)}$ (**3a**)

Bond Lengths (Å)			
Cu−O(2)	2.056(4)	P(1)−C(41)	1.823(4)
Cu−O(3)	2.164(5)	P(1)−C(31)	1.827(4)
Cu−P(2)	2.240(2)	P(1)−C(21)	1.841(3)
Cu−P(1)	2.282(2)	P(2)−C(51)	1.820(4)
O(2)−C(2)	1.293(7)	P(2)−C(71)	1.834(3)
O(3)−C(3)	1.265(8)	P(2)−C(61)	1.836(4)

Bond Angles (deg)			
O(2)−Cu−O(3)	79.3(2)	C(3)−O(3)−Cu	109.5(4)
O(2)−Cu−P(2)	120.82(14)	C(2)−O(2)−Cu	112.4(4)
O(3)−Cu−P(2)	109.2(2)	C(21)−P(1)−Cu	116.4(2)
O(2)−Cu−P(1)	109.82(14)	C(41)−P(1)−Cu	115.6(2)
O(3)−Cu−P(1)	100.7(2)	C(31)−P(1)−Cu	114.3(2)
P(2)−Cu−P(1)	124.50(7)	C(51)−P(2)−Cu	119.2(2)
C(71)−P(2)−Cu	117.5(2)	C(61)−P(2)−Cu	110.2(2)
O(2)−C(2)−C(1)	122.6(6)	O(3)−C(3)−C(4)	121.6(6)
O(2)−C(2)−C(3)	118.8(6)	O(3)−C(3)−C(2)	119.5(6)

$\mathrm{P_{av}} = 2.261(2)$ Å] than those in $\mathrm{[Cu(PPh_3)_2(PhenSQ)]}$ [Cu−$\mathrm{P_{av}} = 2.240(3)$ Å] and in $\mathrm{[Cu(PPh_3)_2(4\text{-}NO_2C_6H_4CO_2)]}$ [Cu−$\mathrm{P_{av}} = 2.237(1)$ Å].[72]

$\mathrm{Cu(PPh_3)_2}$(*O*-bs). Crystallographic characterization of **4a** has shown that it contains two slightly different $\mathrm{Cu(PPh_3)_2}$(*O*-bs) molecules with a distorted tetrahedral geometric arrangement as shown in Figure 2, with selected bond lengths and bond angles listed in Table 6.

The elemental cell contains four molecules of $\mathrm{[Cu(PPh_3)_2}$-(*O*-bs)], of which two are identical and show slight differences in bond distances and angles compared to the others as shown in Figure 2 (molecules 1 and 2). In both molecules the carboxylato group of the O-benzoylsalicylate ligand is bidentate with somewhat different [2.226(2) and 2.280(2) Å] and very similar [2.148(2) and 2.183(2) Å] Cu−O distances. The Cu−P distances are close in both molecules 1 and 2 [Cu−$\mathrm{P_{av}} =$ 2.2326(6) (molecule 1) and 2.2398(6) Å (molecule 2)]. This fits well to Cu−$\mathrm{P_{av}}$ distances in $\mathrm{[Cu(PPh_3)_2(4\text{-}NO_2C_6H_4CO_2)]}$ [2.237(1) Å].[72] The carboxylate bite is 59.16(6)° compared to 58.9(1)° in $\mathrm{[Cu(PPh_3)_2(4\text{-}NO_2C_6H_4CO_2)]}$,[72] and all other angles involving the Cu atom are close to that of a regular tetrahedron. The overall feature of the structures suits the general geometry of a distorted tetrahedron as found earlier for mononuclear copper(I) carboxylates.[73−75]

Table 6. Selected Bond Lengths and Angles for $\mathrm{Cu(PPh_3)_2}$(*O*-bs)·$\mathrm{CH_3COCH_3}$ (**4a**·$\mathrm{CH_3COCH_3}$)

Bond Lengths (Å)			
Cu(1)−O(10)	2.148(2)	C(10)−C(11)	1.513(3)
Cu(1)−P(1)	2.2262(6)	O(13)−C(17)	1.205(3)
Cu(1)−P(2)	2.2389(6)	O(11)−C(10)	1.244(3)
Cu(1)−O(11)	2.280(2)	O(10)−C(10)	1.250(3)
P(1)−C(1A)	1.826(2)	P(2)−C(5A)	1.824(2)
P(1)−C(3A)	1.825(2)	P(2)−C(4A)	1.821(2)
P(1)−C(2A)	1.829(2)	P(2)−C(6A)	1.821(2)
Cu(2)−O(20)	2.183(2)	C(20)−C(21)	1.510(3)
Cu(2)−O(21)	2.226(2)	O(20)−C(20)	1.246(3)
Cu(2)−P(3)	2.2360(6)	O(23)−C(27)	1.212(4)
Cu(2)−P(4)	2.2435(6)	O(21)−C(20)	1.245(3)
P(3)−C(8A)	1.827(2)	P(4)−C(12A)	1.828(2)
P(3)−C(9A)	1.829(2)	P(4)−C(11A)	1.824(2)
P(3)−C(7A)	1.830(2)	P(4)−C(10A)	1.811(2)

Bond Angles (deg)			
O(10)−Cu(1)−P(1)	119.68(5)	O(11)−C(10)−O(10)	122.8(2)
O(10)−Cu(1)−P(2)	110.01(5)	O(10)−C(10)−C(11)	118.3(2)
P(1)−Cu(1)−P(2)	129.06(2)	C(10)−O(11)−Cu(1)	86.12(13)
P(1)−Cu(1)−O(11)	106.59(5)	O(10)−Cu(1)−O(11)	59.16(6)
P(2)−Cu(1)−O(11)	107.72(5)	C(10)−O(10)−Cu(1)	91.95(14)
C(6A)-P(2)−Cu(1)	113.77(7)	C(1A)-P(1)−Cu(1)	116.46(7)
C(4A)-P(2)−Cu(1)	119.34(7)	C(2A)-P(1)−Cu(1)	111.44(7)
C(5A)-P(2)−Cu(1)	111.21(7)	C(3A)-P(1)−Cu(1)	115.24(7)
O(20)−Cu(2)-O(21)	59.42(6)	C(20)−O(21)−Cu(2)	87.86(14)
O(20)−Cu(2)−P(3)	119.20(5)	C(20)−O(20)−Cu(2)	89.82(14)
O(21)−Cu(2)−P(3)	108.40(5)	O(21)−C(20)−O(20)	122.6(2)
O(20)−Cu(2)−P(4)	109.31(5)	O(20)−C(20)−C(21)	118.5(2)
O(21)−Cu(2)−P(4)	111.96(5)	P(3)−Cu(2)−P(4)	127.86(2)
C(8A)-P(3)−Cu(2)	110.13(7)	C(10A)-P(4)−Cu(2)	111.67(8)
C(9A)-P(3)−Cu(2)	118.11(7)	C(11A)-P(4)−Cu(2)	112.86(7)
C(7A)-P(3)−Cu(2)	115.97(7)	C(12A)-P(4)−Cu(2)	119.94(7)

Kinetic Measurements. $\mathrm{Cu(PPh_3)_2(fla)}$ forms stable solutions at room temperature in DMF under dinitrogen or argon but under dioxygen slow oxygenation occurs. The kinetics of the oxygenation was followed by determining the concentration of $\mathrm{Cu(PPh_3)_2(fla)}$ in the reaction solutions as a function of time by electron spectroscopy at 430.5 nm. Experimental conditions are summarized in Table 3. The measured absorption spectra for $\mathrm{Cu(PPh_3)_2(fla)}$ dissolved in DMF (7.57×10^{-4} M) at 363.16 K are shown in Figure 3, with time range being 6 h.

To determine the rate dependence on the two reactants, oxygenation runs were performed at different dioxygen pressures (Table 3, experiments 1−7) and various initial $\mathrm{Cu(PPh_3)_2(fla)}$ concentrations (Table 3, experiments 8−12). A simple rate law for the reaction between $\mathrm{Cu(PPh_3)_2(fla)}$ and $\mathrm{O_2}$ is as shown in eq 3.

$$\begin{aligned}-\mathrm{d}[\mathrm{Cu(PPh_3)_2(fla)}/\mathrm{d}t &= \mathrm{d}[\mathrm{Cu(PPh_3)_2}(O\text{-}\mathrm{bs})]/\mathrm{d}t \\ &= k[\mathrm{Cu(PPh_3)_2(fla)}]^m[\mathrm{O_2}]^n \qquad (3)\end{aligned}$$

Under pseudo first-order conditions at constant dioxygen concentration (keeping dioxygen pressure constant) for the experiments the concentrations of $\mathrm{[Cu(PPh_3)_2(fla)]}$ were measured. A typical time course and first-order plot of the oxygen-

---

(72) Cabras, M. A.; Naldini, L.; Zoroddu, M. A.; Cariati, F.; Demartin, F.; Masciocchi, N.; Sansoni, M. *Inorg. Chim. Acta* **1985**, *104*, L19.

(73) Mehrotra, R. C.; Bohra, R. *Metal Carboxylates*; Academic Press: London, 1983; pp 286−295.

(74) Párkányi, L.; Speier, G. *Z. Kristallogr.* **1995**, *210*, 307.

(75) Speier, G.; Selmeczi, K.; Pintér, Z.; Huttner, G.; Zsolnai, L. *Z. Kristallogr.* **1998**, *213*, 263.

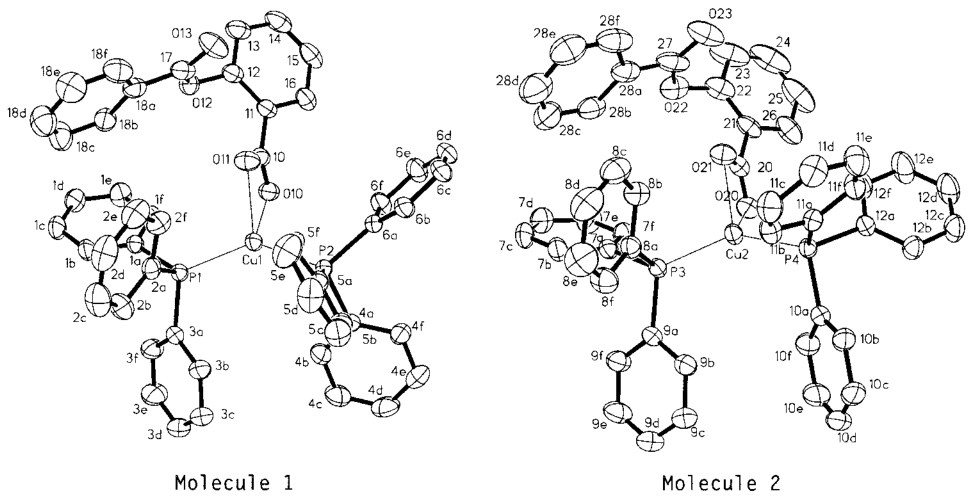

Figure 2. Molecular structure and atomic numbering scheme for $Cu(PPh_3)_2(O\text{-bs})\cdot CH_3COCH_3$ (**4a**$\cdot CH_3COCH_3$). Ellipsoids are drawn at the 50% probability level.

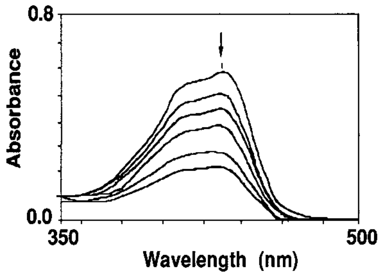

Figure 3. Spectral changes accompanying the oxygenation of $Cu(PPh_3)_2$(fla) during experiment 9 in Table 3. For simplicity only a few spectra are shown, taken at 0, 65, 125, 185, 340, and 455 min.

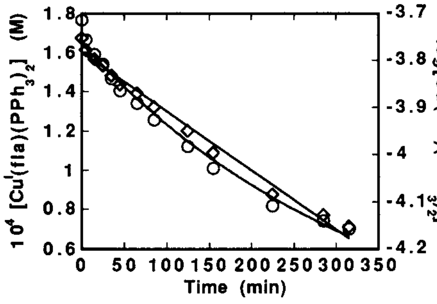

Figure 4. The time course for oxygenation of $Cu(PPh_3)_2$(fla) monitored at 430.5 nm (○), and plot of log[$Cu(PPh_3)_2$(fla)] versus reaction time for the oxygenation of $Cu(PPh_3)_2$(fla) (experiment 4, Table 3) (◇).

ation of $Cu(PPh_3)_2$(fla) is shown in Figure 4 for experiment 4; the reaction remains first order in $Cu(PPh_3)_2$(fla) for the whole time in which the experiment was followed (62% conversion, 5.2 h). The first-order dependence of the reaction rate on $Cu(PPh_3)_2$(fla) could be also confirmed by plotting the initial reaction rate $-d[Cu(PPh_3)_2(fla)]/dt$ versus substrate concentration (Table 3, experiments 8−12). The straight line so obtained as shown in Figure 5 validates the first-order dependence in $Cu(PPh_3)_2$(fla) with a slope $k' = (2.58 \pm 0.27) \times 10^{-5}$ s^{-1} and a correlation coefficient of 97.38%. Columns k, k' (k' = pseudo-first-order rate constant), and R in Table 3 report the slopes and correlation coefficients obtained from least-squares method for these linear regressions.

Experiments made at different dioxygen pressures (0.022, 0.040, 0.067, 0.092, 0.106, 0.120, and 0.148 MPa) show that P_{O_2} appreciably influences the rate of the reaction (Table 3, experiments 1−7). Kinetic measurements of the reaction rate with respect to the dioxygen concentration indicate a first order

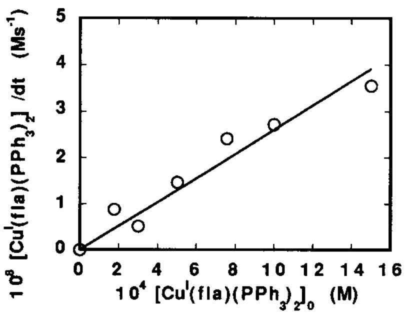

Figure 5. Plot of initial oxygenation rate of $Cu(PPh_3)_2$(fla) versus the initial $Cu(PPh_3)_2$(fla) concentration (experiments 4, 8−12, Table 3).

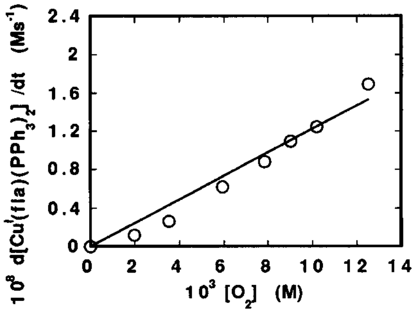

Figure 6. Plot of $d[Cu(PPh_3)_2(fla)]/dt$ versus O_2 pressure for experiments 1−7 in Table 3.

dependence. A plot of $-d[Cu(PPh_3)_2(fla)]/dt$ versus [O_2] for the above experiments gave a straight line with a slope of $k[Cu(PPh_3)_2(fla)] = (1.22 \pm 0.11) \times 10^{-6}$ s^{-1} and a correlation coefficient of 99.34% (Figure 6).

On the basis of the results above, one can conclude that the reaction follows rate law (3) with $m = n = 1$, from which a mean value of the kinetic constant k of $4.16 \pm 0.48 \times 10^{-3}$ mol L^{-1} s^{-1} at 363.16 K was obtained (Table 3).

The activation parameters for the present oxygenation reaction were determined from the temperature dependence of the kinetic constant k. The temperature-dependent reaction rate measurements in the range of 363.16−393.16 K (experiments 1−12, 13, 14, and 15 in Table 3) resulted in a straight line in the Eyring plot (Figure 7), with a correlation coefficient of 99.5% and activation parameters $\Delta H^{\ddagger} = 102 \pm 7$ kJ mol^{-1}, $\Delta S^{\ddagger}$ (363.16 K) $= -13 \pm 21$ J mol^{-1} K^{-1}, and $\Delta G^{\ddagger}$ (363.16 K) $= 106 \pm 14$ kJ mol^{-1}, respectively. Reaction rates on the oxygenation of 4′-substituted flavonolato copper complexes $Cu(PPh_3)_2(4'R\text{-fla})$

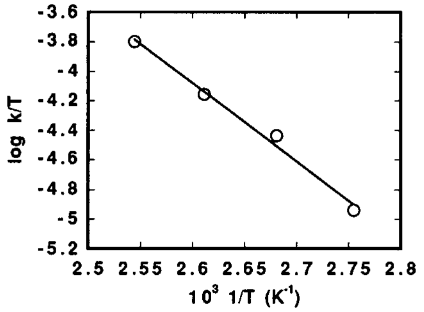

Figure 7. Eyring plot of rate constant, *k*, for the oxygenation of $Cu(PPh_3)_2(fla)$.

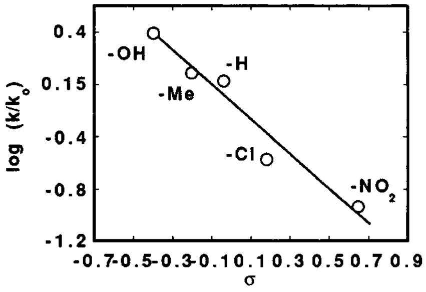

Figure 8. Hammett plot for the oxygenation of $Cu(PPh_3)_2(4'\text{-R-fla})$ complexes.

(**3a**−**e**) (eq 4) under identical conditions were determined (with various electron-withdrawing or releasing substituents R) in order to find out electronic effects on the reaction rate.

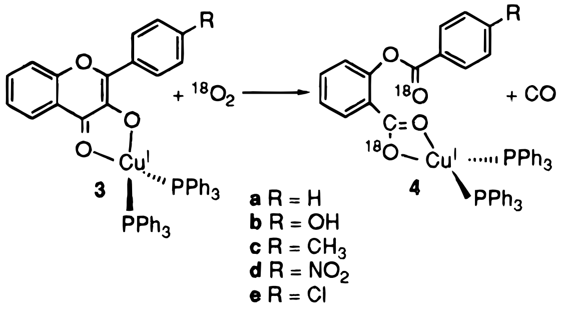

(4)

The Hammett plot obtained is shown in Figure 8. Electron realizing substituents enhanced the reaction rate, and the reaction constant ρ was found to be −1.32.

$^{18}O_2$ Labeling Experiments. Oxygenation of flavonolatobis(triphenyl phosphine) copper(I) was also carried out with a mixture of $^{16}O_2$ and $^{18}O_2$ (4:1). After 20 h of stirring the reactants at 25 °C, GLC-MS analysis of the gas phase showed only the presence of unlabeled CO. The pale yellow solution was evaporated to dryness, giving a mixture of $Cu(PPh_3)_2(^{16}O\text{-bs})$ and $Cu(PPh_3)_2(^{18}O\text{-bs})$: IR (Nujol) $\nu(C^{18}O)$ 1714 cm^{-1}, $\nu(C^{16}O^{18}O)$ 1514, 1364 cm^{-1}, $\nu(C^{16}O)$ 1734 cm^{-1}, $\nu(C^{16}O_2)$ 1547, 1380 cm^{-1}. The GLC-MS analysis of the residue, after treated with Etheral diazomethane, shows the presence of ^{16}O- and ^{18}O-benzoylsalicylic acid methyl ester in the appropriate ratio: *m/z* 260(M$^+$, 0.4), 256(M$^+$, 1.8), 229(0.11), 227(0.17), 225(1.0), 107(25), 105(100). The ^{18}O-benzoylsalicylic acid derivative gave a molecular ion at *m/z* 260 (256 + 4; $C_{15}H_{12}{}^{16}O_2{}^{18}O_2$), showing that both ^{18}O atoms of $^{18}O_2$ are incorporated into the carboxylic acid from molecular oxygen. The relative abundance of *m/z* 260 to that at *m/z* 256 parallels the $^{18}O_2$ enrichment used in the experiment. The same is observed for the base peak, *m/z* 107 (105 + 2). Instead of the peak at *m/z* 225 (M − 31), peaks at 227 (M − 33) and 229 (M − 31) are present.

Scheme 2

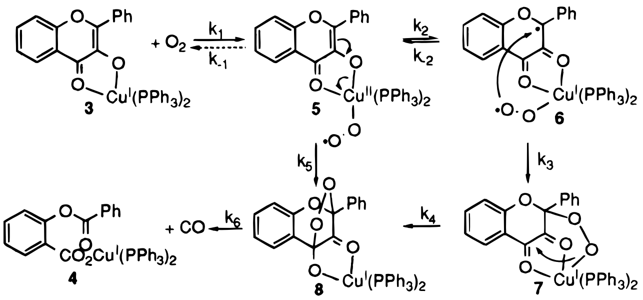

Discussion

All of the experimental data reported in the previous sections can be used for the interpretation of the mechanism of copper(I) assisted oxygenolysis of coordinated flavonolate to *O*-benzoylsalicylate. Dioxygenase enzymes seem to have reactive substrates, and copper(I) complexes have a rich dioxygen chemistry.[76,77] One can put the question forward: what is the role of the metal? The requirement of a redox metal at the active site of the enzymes, e.g., iron or copper, may have the function either to activate dioxygen and/or activate the substrate by changing the electron density either by withdrawing or releasing electrons or just to deprotonate the substrate. In the tetrahedral copper flavonolate complexes **3** the structural data indicate that the electron distribution in the coordinated flavonolate differs only slightly from that of the free ligand. Flavonolate as a chelating ligand forms stable complexes with copper ions. In most cases they are stable toward dioxygen in solid form and even in solution at ambient conditions. The reactivity of copper(I) in **3** is also low due to the stabilizing effect of the phosphine ligands.[78] Compounds **3** are smoothly oxygenated under ambient conditions giving the copper(I) complexes **4** with the new ligand of *O*-benzoylsalicylate formed in the enzyme-like reaction. At elevated temperature the reaction proceeds reasonably fast. However it is interesting to note that copper(I) is not oxidized to copper(II) even under more severe conditions, and the geometry around the copper is tetrahedral as found by other mononuclear copper(I) carboxylate complexes.[73−75]

$^{18}O_2$ labeling experiments on the oxygenation of **3a** revealed that both ^{18}O-atoms of the $^{18}O_2$ molecule are incorporated into the substrate and the extruded carbon monoxide does not contain ^{18}O, mimicking the enzyme action (eq 4).[38]

A reaction mechanism that nicely fits the chemical, spectroscopic, labeling, kinetic, and thermodynamic data is shown in Scheme 2. Kinetic studies on the oxygenation of the flavonolato complexes **3** established a second-order overall rate expression, indicating that the rate-determining step must be bimolecular, namely the reaction of **3** with dioxygen or a unimolecular process such as the formation of the trioxametallocycle (**7**) or the endoperoxide (**8**). The intramolecular electron shift **5** ⇌ **6** is probably very fast, but either k_3 or k_4 may be rate-determining. In the latter case the dioxygen-uptake is a fast preequilibrium, and the formation of the trioxametallocycle (**7**) or the endoperoxide (**8**) is the rate-determining step. Both mechanistic assumptions satisfy the kinetic data, but we believe that the

---

(76) Kitajima, N.; Moro-oka, Y. *Chem. Rev.* **1994**, *94*, 737.

(77) Tyeklár, Z.; Karlin, K. D. *Acc. Chem. Res.* **1989**, *22*, 241.

(78) Hathaway, B. J. In *Comprehensive Coordination Chemistry*; Wilkinson, G., Gillard, R. D., McCleverty, J. A., Eds.; Pergamon Press: Oxford, 1987; Vol. 5, p 536.

bimolecular reaction between **3** and O_2 is more probably the slow step. The following data favor this assumption. The moderate negative $\Delta S^{\ddagger}$ value (-13 ± 21 J mol^{-1} K^{-1}) of the oxygenation step favors a bimolecular reaction, despite the fact that this value is somewhat less than expected for a bimolecular step from theoretical considerations.[79] This is also supported by the Hammett correlation (Figure 8, Table 7), which stresses that the higher electron density on the copper results in higher reaction rates. The crucial evidence for a bimolecular reaction step is the reaction constant ρ, which was found to be -1.32. This value is very similar to that we have found earlier for the oxygenation of CuCl in pyridine ($\rho = -1.24$),[80] and this indicates an electrophilic attack of dioxygen on copper(I). Mononuclear superoxo copper(II) complexes have been prepared and characterized already, and their high reactivity has been demonstrated.[81−84] Further possible fast reaction steps of the copper(II) superoxide complex **5** leading to the endproduct **4** are as shown in Scheme 2. It is reasonable to assume steps that may require an electron flow from the flavonolato ligand to copper(II) in **5**, resulting in the copper(I) superoxide complex **6** with flavonolate radical coordinated to the copper ion. This is then converted via an intramolecular radical radical reaction to the trioxametallocycle **7**. A deprotonated 2-hydroperoxide **7** is able to attack the 4-C=O carbon in a nucleophilic attack to form the copper(I) endoperoxide complex **8**. A breakdown of **8** with concomitant loss of CO results in the final product, *O*-benzoylsalicylatobis(triphenylphosphine)copper(I) (**4**). The mechanism of the breakdown of the endoperoxide is not known and to our knowledge no investigations have been done on this type of reactions.[85] A homolytic cleavage of the O−O bond seems to be reasonable, followed by the extrusion of carbon monoxide. The breakdown of this type of endoperoxides (**9**) to the metal complex of O-benzoylsalicylate (**10**) (eq 5) shows some formal similarities to the transformation of trioxametallacycles (**11**) to anhydrides and oxometal compounds (eq 6) proposed for catechol dioxygenase mimicking reactions, as adapted from the Criegee-type rearrangement of peroxides.[86]

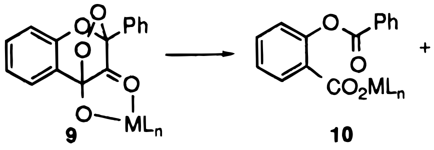

(5)

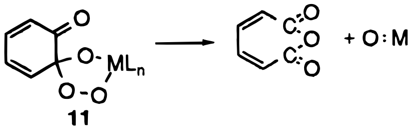

(6)

The exact nature of this rearrangement is not known, but the first step is probably the homolytic scission of the O−O bond[87] followed by the CO elimination step. More research is necessary for the clarification of this type of cleavage mechanism.

Table 7. Hammett Data for the Oxygenation of Cu(PPh$_3$)$_2$(4′-R-fla)

complex	R	σ	10^2k, s^{-1} mol L^{-1}
3a	H	0.000	6.291
3b	OH	−0.370	15.138
3c	Me	−0.170	7.270
3d	NO$_2$	0.710	0.625
3e	Cl	0.227	1.497

A [3 + 2] dipolar addition of triplet dioxygen to the coordinated flavonolate ligand, as a formal alternate reaction path, seems highly improbable for the cyclic endoperoxide **8** and can be excluded for several reasons (thermodynamic and symmetry considerations). Thus stepwise formation of the endoperoxide **8** from the dioxygen adduct may be concluded with certainty. The nucleophilic attack of the bound peroxide could, however, also take place on the 3-C=O group as well, giving rise to a 1,2-dioxetane intermediate. The absence of chemiluminescence during the reaction, which is very characteristic for the decomposition of 1,2-dioxetanes to carbonyl compounds, seems to render this pathway unlikely.[88−91] This may be due to less steric strain in the five-membered cyclic peroxide compared to that in the four-membered 1,2-dioxetane, or may have also an electronic explanation due to higher electron density on the 3-C=O carbon than in the case of 4-C=O carbon accessible in the nucleophilic attack. Unfortunately, efforts to isolate the peroxide species in the oxygenation reactions at ambient conditions failed. This supports the assumption in the mechanism that either steps after the formation of **5** are fast or one of the following steps leading to transformation of **5** to the endoperoxide is rate-limiting.

So far the role of copper ion in these oxygenation reactions is difficult to assess with certainty. Flavonolate ion can be oxygenated under protic conditions[42] or by the use of singlet oxygen[44] to *O*-benzoylsalicylate. In the oxygenation of Co(fla)(salen) complexes dissociation of the flavonolate ion from the cobalt has been proved, and the reaction between the free ligand and dioxygen assumed.[48] Nonetheless we believe that the copper ions in the enzyme and also in model reactions act as an electron buffer, due to their ability to accept or donate electrons. In this sense the reactivity of the flavonolato ligand is transformed to a radical anion, and the copper(I) formed can activate dioxygen. It is important however to tress that oxygenation studies to further copper-based model reactions are necessary to elucidate these points, and the interception of some of the peroxide species is necessary to have a clearer picture of the mechanism of the oxidative scission reaction and especially of the role of copper in these reactions. We aware of the fact that similar studies on models with copper(II) ions will be more apropiate, since that matches better the situation in the enzyme; however, if redox changes of the metal ion are important then the redox equilibria may be similar not depending on the starting complex.

Acknowledgment. We thank Dr. G. Szalontai for help with NMR spectra. Financial support of the Hungarian National Research Fund (OTKA T-7443, T-030400, and T-016285) is gratefully acknowledged.

---

(79) Frost, A. A.; Pearson, R. G. *Kinetics and Mechanism. A Study of Homogeneous Chemical Reactions*; John Wiley & Sons: New York, 1961; p 101.

(80) Balogh-Hergovich, É.; Speier, G. *Trans. Met. Chem.* **1982**, *7*, 177.

(81) Harata, M.; Jitsukawa, K.; Masuda, H.; Einaga, H. *J. Am. Chem. Soc.* **1994**, *116*, 10817.

(82) Fujisawa, K.; Tanaka, M.; Moro-oka, Y.; Kitajima, N. *J. Am. Chem. Soc.* **1994**, *116*, 12079.

(83) Harata, M.; Jitsukawa, K.; Masuda, H.; Einaga, H. *Chem. Lett.* **1996**, 813.

(84) Wada, A.; Harata, M.; Hasegawa, K.; Jitsukawa, K.; Masuda, H.; Mukai, M.; Kitagawa, T.; Einaga, H. *Angew. Chem.* **1998**, *37*, 798.

(85) Clennan, E. L.; Foote, C. S. In *Organic Peroxides*; Ando, W., Ed.; Wiley: Chichester, 1992; p 225.

(86) Jefford, C. W.; Cadby, P. A. In *Progress in the Chemistry of Organic Natural Products*; Zechmeister, L., Herz, W., Grisebach, H., Kirby, G. W., Eds.; Springer-Verlag: Wien, 1981; pp 191−265.

(87) Kotsuki, H.; Saito, I.; Matsuura, T. *Tetrahedron Lett.* **1981**, *22*, 469.

(88) Schulz, M.; Kirschke, K. In *Organic Peroxides*; Swern, D., Ed.; Wiley-Interscience: New York, 1972; Vol. III, pp 67−140.

(89) March, J. *Advanced Organic Chemistry*, 4th ed.; Wiley-Intersience: New York, 1992; p 830.

(90) Foote, C. S. *Pure Appl. Chem.* **1971**, *27*, 635.

(91) Kearns, D. R. *Chem. Rev.* **1971**, *71*, 5.

Supporting Information Available: Details of the X-ray structure determination for Cu(PPh_3)$_2$(fla) and Cu(PPh_3)$_2$(*O*-bs)·CH_3COCH_3. This material is available free of charge via the Internet at http://pubs.acs.org. X-ray crystallographic files, in CIF format, for the structure determination of Cu(PPh_3)$_2$(fla) and Cu(PPh_3)$_2$(*O*-bs) are available on the Internet only.

IC990175D